Available online at www.sciencedirect.com

SCIENCE DIRECT®

Bioelectrochemistry 66 (2005) 79–87

Bioelectrochemistry

www.elsevier.com/locate/bioelechem

Polyoxometallates as inorganic templates for electrocatalytic network films of ultra-thin conducting polymers and platinum nanoparticles

Katarzyna Karnicka[a], Malgorzata Chojak[a], Krzysztof Miecznikowski[a], Magdalena Skunik[a], Beata Baranowska[a], Aneta Kolary[a], Aleksandra Piranska[a], Barbara Palys[a], Lidia Adamczyk[b], Pawel J. Kulesza[a,*]

[a]*Department of Chemistry, University of Warsaw, Pasteura 1, PL-02-093 Warsaw, Poland*

[b]*Division of Chemistry, Department of Materials and Process Engineering and Applied Physics, Czestochowa University of Technology, Armii Krajowej 19, PL-42-200 Czestochowa, Poland*

Received 23 March 2004; received in revised form 4 June 2004; accepted 14 June 2004
Available online 25 August 2004

Abstract

We develop a concept of fabrication of the multilayer network films on electrodes by exploring the ability of a Keggin-type polyoxometallate, phosphododecamolybdate ($PMo_{12}O_{40}^{3-}$), to form stable anionic monolayers (templates) on carbon and metals including platinum. By repeated alternate treatments in the solution of $PMo_{12}O_{40}^{3-}$ (or in the colloidal suspension of polyoxometallate-protected Pt-nanoparticles) and in the solution of monomer (e.g. anilinium) cations, the amount of the material can be increased systematically (layer-by-layer) to form stable three-dimensional assemblies on electrode (e.g. glassy carbon) surfaces. In the resulting hybrid (organic–inorganic) films, the layers of negatively charged polyoxometallate, or polyoxometallate-protected (stabilized) Pt-nanoparticles, are linked or electrostatically attracted by ultra-thin layers of such positively charged conducting polymers as polyaniline (PANI), polypyrrole (PPy) or poly(3,4-ethylenedioxythiophene), PEDOT. Consequently, the attractive physicochemical properties of polymers and reactivity of polyoxometallate or noble metal particles are combined. The films are functionalized and show electrocatalytic properties towards reduction of nitrite, bromate, hydrogen peroxide or oxygen. They are of importance to the chemical and biochemical sensing as well as to the biochemical and medical applications.

Keywords: Phosphomolybdate; Self-assembled monolayer; Ultra-thin conducting polymers; Stabilized platinum nanoparticles; Layer-by-layer films; Oxygen reduction; Nitrite and bromate reduction

1. Introduction

During recent years, there has been growing activity in the area of fabrication and characterization of monomolecular (monolayer) and multilayered organized assemblies at solid surfaces that produce functionalized interfaces with well-defined composition, structure, thickness and catalytic reactivity [1]. In this context, a substantial impetus is given to investigations of alkanothiols and their derivatives, which can be successfully employed to obtain dense robust monolayer coverages on gold [1–4]. The self-assembly of ordered organic molecular arrays formed spontaneously as monolayers on solid surfaces or the sequential adsorption of oppositely charged polyelectrolytes are of particular interest to the advanced materials preparation [2–4]. Attractiveness of the self-assembly includes the possibility of controlled formation of any number of layers of different composition on a large variety of substrates. For example, the formation of ultra-thin films and ordered or derivatized assemblies of conjugated polymers [3–9] shall be mentioned. Also, synthesis of nanoparticles and their organization into two-dimensional arrays and three-dimensional networks have prompted the increased interest due to potential applications in many areas including molecular and nanoelectronics [1], sensors [1,10], catalysis and electrocatalysis [11–16]. The

---

* Corresponding author. Tel.: +48 22 8220211; fax: +48 22 8225996.
E-mail address: pkulesza@chem.uw.edu.pl (P.J. Kulesza).

1567-5394/$ - see front matter © 2004 Elsevier B.V. All rights reserved.
doi:10.1016/j.bioelechem.2004.06.005

important issues are means of fabrication, assembly, average size diameter and distribution, as well as electronic properties and reactivity of such nanosized materials [17–20]. Monolayers of alkanothiolates are capable of passivating gold nanoparticles and producing alkanothiolate monolayer protected clusters of gold. An important function of alkanothiolates is to separate the metal (Au) clusters to prevent their agglomeration (i.e. degradation or aging). Self-organization of such clusters into the network films of metal nanoparticles [16–25] is feasible. Such films combine bulk and molecular properties within a nanometer scale material that is expected to yield novel and promising size-dependent electronic, optical and chemical properties.

An important possibility arises from the adsorption or chemisorption of inorganic monolayers (templates) that permits formation of two-dimensional arrays and three-dimensional (layer-by-layer) domains on electrodes [26–41]. Among rigid inorganic templates, polyoxometallates [31–34,36–40] are particularly attractive because of their ability to adsorb irreversibly on solid surfaces. In particular, heteropolyacids of molybdenum and tungsten are characterized by reversible stepwise multi-electron-transfer reactions of importance to electrocatalysis, electrochromism, molecular electronics and sensing. We address here the formation of bilayer and multilayer films composed alternatively from monolayers of phosphododecamolybdate (PMo_{12}) Keggin type anions and conducting polymer, mostly polyaniline (PANI) but also polypyrrole (PPy) and poly(3,4-ethylenedioxythiophene) (PEDOT). PANI is commonly studied due to its well-defined redox properties, good protonic conductivity, in addition to high electronic conductivity, and chemical stability in acid media [42–46]. PPy is often considered for many applications because it is stable and conductive in the broad range of media that include neutral and acid solutions [47]. PEDOT has recently been recognized as exceptionally stable and conductive (in its doped state) organic polymer [48,49]. The layer-by-layer procedure involves polymerization of surface confined monomer ions that have been electrostatically attracted to a negatively charged monolayer of heteropolymolybdate on glassy carbon. The polymerization step is completed electrochemically upon medium transfer to acid electrolyte. By repeated and alternate treatments in the appropriate solutions, the amount of material on the electrode surface can be increased in a controlled manner. The fact that formal potentials of PMo_{12} redox processes lie in the potential range where polymer interlayers are conductive produces a system capable of fast charge propagation.

We also explore here the ability of polyoxometallate (phosphomolybdate) to undergo adsorption and form monolayers on metal (Pt) nanoparticles (ca. 7 nm). Nanoparticles of platinum and its alloys are characterized by high surface area to volume ratios and exhibit promising electrocatalytic properties towards fuels, namely the reduction of oxygen and the oxidation of hydrogen or methanol. However, catalytic reactivity of alkanothiol-protected Pt [50], Au/Pt alloy [51], or alkyl isocyanide-derivatized [52] and mercaptoaniline-functionalized [53] platinum nanoparticles is rather limited. Much more promising for electrocatalysis are colloidal platinum nanoparticles prepared within the environment of mixed metal oxide nanostructures [54]. Introduction of polymer matrices [55,56] tends to improve such physical properties as dispersion, size and morphology of metal particles. Therefore, we fabricate polyoxometallate covered (protected) particles and link them together by ultra-thin conducting polymer (polyaniline) bridges. The growth, surface morphology and electrochemical properties of our three-dimensional network films are examined using cyclic voltammetry, potential step techniques, FTIR spectroscopy and STM. The films produce interfaces with specific electrocatalytic properties towards reduction of nitrite, bromate, hydrogen peroxide, and oxygen.

2. Experimental

Phosphododecamolybdic acid, $H_3PMo_{12}O_{40}$, aniline, pyrrole were obtained from Fluka. 3,4-Dioxyetylenethiophene (EDOT) monomer was kindly donated by Bayer. Platinum black clusters (surface area, 20 m^2 g^{-1}) were obtained from Johnson and Matthew. All other chemicals were reagent grade purity, and they were used as received. Solutions were prepared using doubly distilled and subsequently deionized (Millipore Milli-Q) water. Ultra high purity argon gas was used to deaerate investigated solutions. Experiments were carried out at room temperature (20 ± 2 °C).

Electrochemical measurements were done with CH Instruments (Austin, USA) Model 750 workstation. A standard three-electrode cell was used for the preparation of films and for other electrochemical measurements. The working electrode was a glassy carbon disk (3 mm, diameter) supplied by Bioanalytical Systems (West Lafayette, IN, USA), and the counter electrode was made from Pt wire. Before modification, glassy carbon was subjected to polishing (on a cloth) with successively finer grade aqueous alumina slurries (grain size, 5–0.5 μm). All potentials were expressed versus the saturated (KCl) Ag/AgCl electrode.

Preparation of multilayer films of PMo_{12} and PANI was achieved via the alternate immersion scheme described by us earlier [9]. First, the glassy carbon surface was modified with a self-assembled PMo_{12} monolayer (adsorbate) by dipping it for 10 min in an aqueous solution of 2 mmol dm^{-3} $H_3PMo_{12}O_{40}$. Anilinium (monomer) ions were introduced into PMo_{12} monolayer by exposing the PMo_{12}-modified electrode to a 0.07 mol dm^{-3} solution of aniline in 0.5 mol dm^{-3} H_2SO_4 for 5 min. PANI was electropolymerized by potential cycling (at 50 mV s^{-1}) from -0.1 to 0.85 V in 0.5 mol dm^{-3} H_2SO_4. Ultra-thin PANI layers were formed during positive potential cycles [9]. After each treatment, the electrode was thoroughly rinsed with water.

Fabrication of polypyrrole (PPy) and PEDOT containing films was achieved in a similar manner except that the monomer solution contained 0.1 mol dm^{-3} pyrrole and 0.1 cm^3 EDOT in 10 cm^3 H_2O. The potential range for electropolymerization of PEDOT was from −0.1 to 1.0 V.

Film loadings, expressed as PMo_{12} surface coverages (in mol cm^{-2}), were estimated (upon consideration of the extrapolated baseline) from charges under the system's reduction voltammetric peak recorded at ca 0.2 V at a slow scan rate, 5 mV s^{-1}.

Polyoxometallate-protected platinum nanoparticles were produced as follows. A suspension of a known amount (0.33 g) of Pt black was formed in 2 mmol dm^{-3} aqueous PMo_{12} solution (10 cm^3). The suspension was sonicated for 2 h, left overnight and then centrifuged three to four times until color remained indefinitely yellow (i.e. PMo_{12} was in the oxidized form and did not interact with Pt any more). As a rule, each supernatant solution was removed and replaced with a fresh PMo_{12} solution. Finally, the centrifuging procedure was done with water. It can be expected that, even following centrifuging procedure, protons dissociating from the adsorbed heterpolyacid molecules exist as counter-ions in water (supernatant). The resulting Pt-PMo_{12} colloidal suspension was stable for at least a month.

The network films containing Pt nanoparticles were assembled as mentioned above for the layer-by-layer generation of PMo_{12} and ultra-thin PANI layers except that instead of a simple PMo_{12} solution, the PMo_{12} colloidal suspension of Pt nanoparticles was used. The glassy carbon electrode was serially exposed to Pt-PMo_{12} solution, each time for 30 min, and rinsed with water. By performing additional alternate immersions in the respective solutions, the thicker network film containing Pt nanoparticles can be produced.

Scanning tunneling microscopy (STM) images were obtained ex-situ (in air) using EasyScan Nanosurf (Switzerland) instrument. The tips of Pt/Ir (90/10) wires of 0.25 mm diameter were formed mechanically, and they were used as probes. The scanning was achieved in the constant-current mode at positive sample bias of 50–100 mV and tunneling current of 1–2 nA.

Infrared spectra were measured with Shimadzu 8400 FTIR spectrometer. The Infrared Reflectance Absorption Spectra (IRRAS) were recorded using a Specular Reflectance Accessory Model 500 produced by Spectra Tech. The beam incidence angle was equal to 80° with respect to the surface normal. Typically 500 scans were averaged for a single reflectance spectrum.

3. Results and discussion

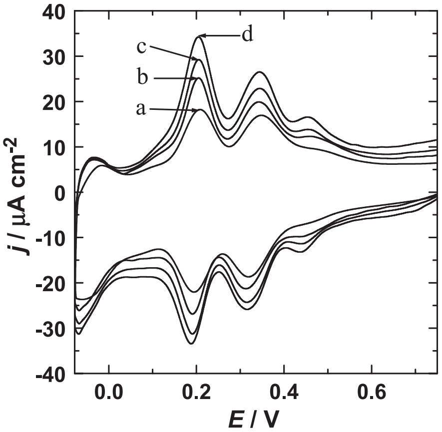

Fig. 1. Cyclic voltammetric responses of (a) glassy carbon electrode modified with PMo_{12} monolayer, and (b–d) after processing through one to four cycles of alternate treatments in 2 mmol dm^{-3} PMo_{12} and 0.07 mol dm^{-3} aniline (0.5 mol dm^{-3} H_2SO_4). Electrolyte, 0.5 mol dm^{-3} H_2SO_4. Scan rate, 50 mV s^{-1}.

Fig. 1 illustrates the layer-by-layer growth of a multilayer hybrid film consisting of PMo_{12} and PANI. An increase of voltammetric peak currents occurs following alternate treatments in PMo_{12} and monomer solutions (the latter step is coupled with interfacial electropolymerization of PANI) as described in Experimental. The initial cyclic voltammogram (Fig. 1, Curve a) shows a typical response (in an anilinium-free H_2SO_4) of a glassy carbon electrode modified with a monolayer of PMo_{12}. The charges under two reduction peaks appearing at potentials ca. 0.32 and 0.18 V (Fig. 1, Curve a) are approximately equal. Also the respective ratios of oxidation-to-reduction peak currents are close to unity. The third set of peaks, though still well-defined, is somewhat less reversible. In view of the literature reports [31–34], the above redox reactions shall be interpreted in terms of three consecutive two-electron processes that can be described as follows:

$$PMo^{VI}_{12}O^{3-}_{40} + ne^- + nH^+ \Longleftrightarrow H_nPMo^{V}_{n}Mo^{VI}_{12-n}O^{3-}_{40} \qquad (1)$$

where n is equal to 2, 4 or 6.

Judging from the charge under the second cathodic peak at 0.18 V (Fig. 1, Curve a), the surface coverage of PMo_{12} is on the level 2×10^{-10} mol cm^{-2} that is, as we discussed earlier [9], equivalent to approximately a monolayer of PMo_{12}. The detailed description of PMo_{12} monolayer chemisorbed on glassy carbon was a subject of our separate work [9]. Each additional voltammogram (Curve b, c or d in Fig. 1) corresponds to the film response upon formation of a superadded PMo_{12}/PANI bilayer. It seems plausible to attribute the most positive set of peaks appearing in the multilayer film at about 0.43 V (Fig. 1, Curve d) to the electroactivity of PANI, namely to the redox behavior of its partially oxidized form emeraldine [42–44]. As in the case of a PMo_{12} monolayer (Fig. 1, Curve a), the cathodic peak that appears at about 0.32 V in Curves b–d (Fig. 1) must be related to the first (most positive) two-electron reduction of PMo_{12}. The fact that this peak is larger than the peak at ca. 0.18 V (Fig. 1, Curve d) originates from the overlapping of the second two-electron reduction of PMo_{12} with the PANI reaction, namely reduction of emeraldine to leucoemeraldine [9]. It is likely that, due to good mediation capabilities of PMo$_{12}$, the redox behavior of ultra-thin PANI interlayers is more redox facile when compared to the typical behavior of conventional PANI film [42–44]. The reversible behavior of ultra-thin PANI film was also observed when it was fabricated on the organic self-assembled alkanothiolate monolayer [5].

The presence of PMo$_{12}$ within the composite film is also evident from the ex-situ FTIR (Fig. 2) examination (by reflectance) of the glassy carbon electrode surface modified with a thin hybrid film of PMo$_{12}$/PANI (Curve a). To confirm the presence of PMo$_{12}$, comparison is made to the spectrum characteristic of PMo$_{12}$ in KBr (Curve b). Although the IR transmittance and reflectance spectra are different when it comes to the comparison of the band intensities, the comparison of band positions (to describe the interactions between PMo$_{12}$ and PANI) is feasible. Despite some overlap from PANI bands in the region from 800 to 1100 cm^{-1}, it is reasonable to expect that bands at 1062, 959 and 887 and 813 cm^{-1} (Curve a) originate from PMo$_{12}$. Since they are somewhat distorted and shifted in comparison to the data of PMo$_{12}$ in KBr (namely to bands in Fig. 2b at 1064, 961, 869 and 787 cm^{-1} characteristic of P–O, Mo=O(terminal), Mo–O(corner sh)–Mo and Mo–O(edge sh)–Mo stretching vibrations [39,57], respectively), strong interaction between heteropolyanion and polymer backbone can be postulated. The spectrum (Curve a) shows also bands in the region 1100–1600 cm^{-1} corresponding to the polymer (PANI) matrix in its emeraldine form [39].

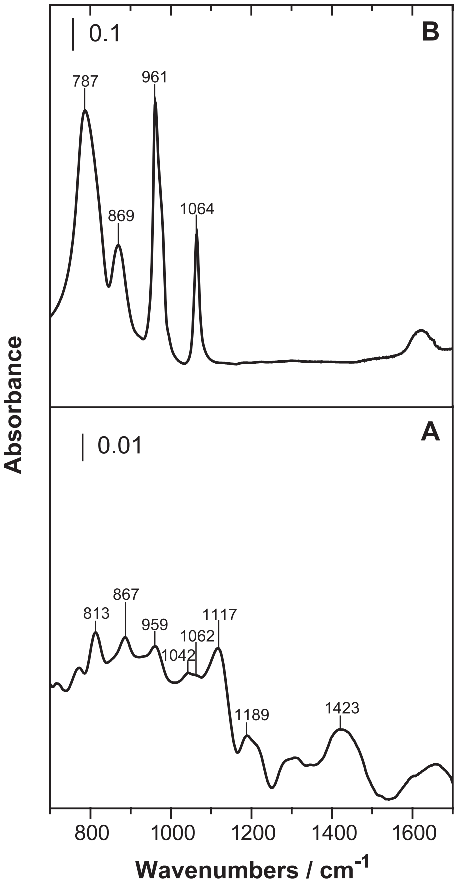

Fig. 2. FTIR spectra of (A) multilayer PMo$_{12}$-PANI hybrid film on glassy carbon (by reflectance) and (B) phosphododecamolybdic acid in KBr.

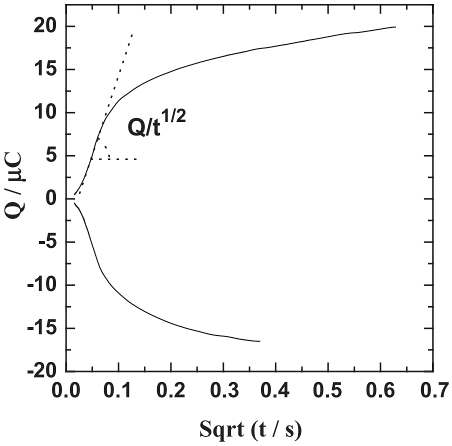

Fig. 3. Double potential step chronoculometric plot for PMo$_{12}$-PANI film deposited on glassy carbon. An initial potential step was from 0.6 to 0.25 V (Fig. 1). Electrolyte, 0.5 mol dm^{-3} H$_2$SO$_4$.

To get some insight into dynamics of charge transport, we also performed a series of chronoculometric (potential step) experiments in which effective (apparent) diffusion coefficients (D_{eff}'s) were estimated by usual means, i.e. from the slopes of dependencies of charge (Q) versus square root of time ($t^{1/2}$) and using integrated Cottrell equation [58,59]:

$$Q/t^{1/2} = 2nF\pi^{1/2}r^2D_{\text{eff}}^{1/2}C_{\text{o}} \tag{2}$$

where r stands for the electrode (disk) radius and other parameters have usual significance. As it comes from the chronoculometric plot (Fig. 3) for the hybrid PMo$_{12}$/PANI film (as for Fig. 1d), the linear portion of the plot is well-defined, and determination of the $Q/t^{1/2}$ slope is feasible. The concentration of PMo$_{12}$ redox (C_{o}) centers was estimated to be on the level 0.6–0.8 mol dm^{-3} upon consideration of such parameters as the PMo$_{12}$ loadings of a series of the hybrid films of different thicknesses (determined from profilometry). Despite some uncertainty in the estimation of C_{o}, it is reasonable to expect D_{eff} to be on the level 1–2 10^{-8} cm^2 s^{-1} for the first most positive PMo$_{12}$ redox reaction in the hybrid film. Certainly, the fast dynamics of charge transport in our composite system is facilitated not only by the high self-exchange rate between PMo$_{12}$ redox centers but also by the fact that the PMo$_{12}$ redox process lies in the potential range where polyaniline is conductive.

The concept of fabrication of hybrid films in a controlled manner using the layer-by-layer approach is not only limited to the PMo$_{12}$/PANI multilayer system. Fig. 4 illustrates the growth of films by alternate immersions in the solutions of PMo$_{12}$ and (A) pyrrole or (B) EDOT monomers. Con-

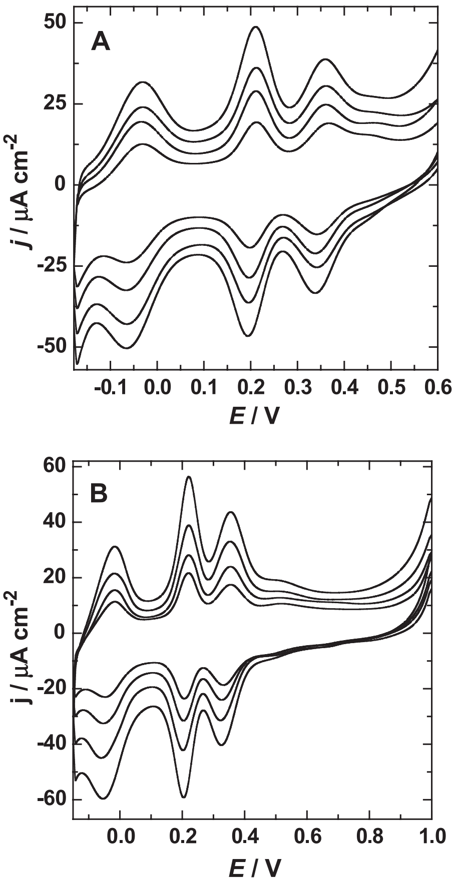

Fig. 4. Cyclic voltammograms of hybrid (A) PMo_{12}-PPy and (B) PMo_{12}-PEDOT films recorded after processing through alternate treatments in PMo_{12} and 0.5 mol dm^{-3} H_2SO_4 solutions of (A) pyrrole or (B) EDOT (as described in Experimental). Electrolyte, 0.5 mol dm^{-3} H_2SO_4. Scan rate, 50 mV s^{-1}.

sequently, the following multilayer films, PMo_{12}/PPy (Fig. 4A) and PMo_{12}/PEDOT (Fig. 4B), have been produced. The cyclic voltammograms shown in Fig. 4 correspond to the film responses (recorded in H_2SO_4 supporting electrolyte) during the growth of respective films, namely following formation (superposition) of additional PMo_{12}/PPy (A) or PMo_{12}/PEDOT (B) bilayers. The electrochemical responses of both PMo_{12}/PPy and PMo_{12}/PEDOT multilayer films are well-defined and reversible. In both cases, a conducting polymer can serve as a robust, conductive, matrix for such polynuclear mixed-valence inorganic system as PMo_{12}. The composite materials have been stabilized due to the existence of electrostatic attraction between anionic PMo_{12} units and positively charged conducting polymer (oxidized) [60]. For PMo_{12}/PEDOT, the effective diffusion coefficients were found on the level 4×10^{-8} cm^2 s^{-1}. The systems are of potential importance to the fabrication of composite (hybrid) films that are capable of effective accumulation and propagation of charge in redox capacitors [61]. Further research is along this line.

We also demonstrate that PMo_{12}/PANI hybrid films exhibit electrocatalytic properties towards reduction of such important analytes as nitrite and bromate (Fig. 5). We explore here the ability of the partially reduced polyoxometallates (heteropolyblues) and metal oxides (bronzes) of molybdenum and tungsten to catalyze the reduction of nitrite, bromate and related electrochemically inert anions [34,62–64]. Curves a in Fig. 5A and 5B stand for the responses of a hybrid PMo_{12}/PANI film in supporting electrolyte (H_2SO_4) only. Curves b and c have been recorded in the presence of nitrite (Fig. 5A) and bromate (Fig. 5B) at two different concentrations. It is noteworthy that the glassy carbon substrate barely shows any electrocatalytic reactivity towards reduction of nitrite (Inset to Fig. 5A) or bromate [62]. The data of Fig. 5 are consistent with the increasing electrocatalytic reactivity of PMo_{12} redox centers with the degree of their reduction. Although the system is not optimum here, at least in terms of the choice of conducting polymer matrix, the research seems to be of importance to the development of electrocatalytic (e.g. amperometric) sensors for inert inorganic anions.

Recently, we have demonstrated that PMo_{12} undergoes strong chemisorption on platinum electrodes as well [65,66]. We have also found that PMo_{12} undergoes similar adsorption at monolayer level on nanosized Pt (platinum black). The procedure of stabilizing of Pt nanoparticles by modification with monolayers of PMo_{12}

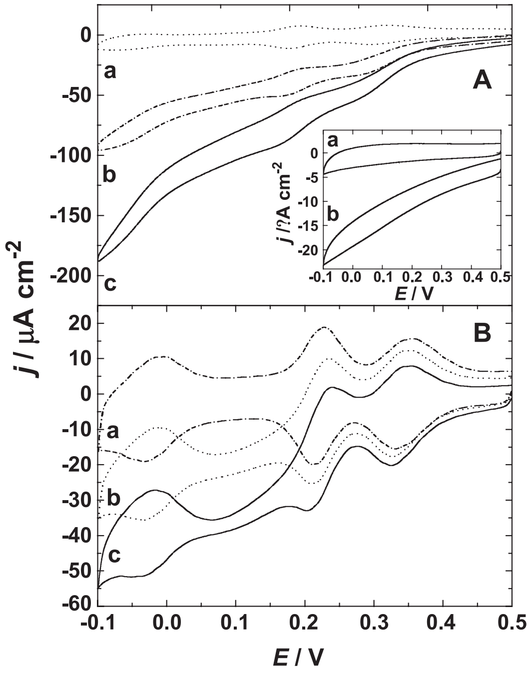

Fig. 5. Electrocatalytic reduction of (A) nitrite and (B) bromate at the glassy carbon electrode modified with PMo_{12}-PANI film. Curves (a) illustrate voltammograms recorded in the electrolyte, 0.5 mol dm^{-3} H_2SO_4, only. Curves (b) and (c) stand for responses in the presence of 10 and 20 mmol dm^{-3} nitrite (A) or bromate (B), respectively. Inset illustrates (a) the voltammetric resposne of the glassy carbon substrate in the supporting electrolyte, and (b) the reduction of nitrite (10 mmol dm^{-3}) at bare glassy carbon. Scan rate, 50 mV s^{-1}.

anions involves conditioning of the Pt clusters in PMo_{12} solution, centrifuging and rinsing aiming at the formation of a colloidal suspension of nanosized platinum in water. An important issue is the existence of electrostatic repulsive interactions between the negatively charged PMo_{12} monolayers on the Pt surfaces: they prevent agglomeration and permit formation of stable colloidal solutions of thus stabilized Pt nanoparticles. Fig. 6 (Curve a) shows a cyclic voltammetric response (recorded in argon-saturated 0.5 mol dm^{-3} H_2SO_4) of a glassy carbon electrode modified with an ultra-thin of PMo_{12}-protected Pt nanoparticles. The spontaneous deposition of such Pt particles on glassy carbon was achieved by simple dipping of the electrode substrate in the PMo_{12}-stabilized suspension. The voltammetric pattern of Fig. 6, Curve a exhibits both the peaks characteristic of PMo_{12} (from 0.1 to 0.45 V) and the proton discharge current that is due to the presence of catalytic Pt at potentials more negative than −0.15 V. In order to get information about dispersion of the platinum nanodeposits on glassy carbon, we have examined the electrode surface by STM (Fig. 7). The uniformly and densely dispersed light spots shall be attributed to the nanostructured platinum. Careful examination of the STM data implies that platinum particles are typically on the level 7–10 nm. Finally, as it comes from the cyclic voltammogram recorded in air saturated H_2SO_4 solution (Fig. 6, Curve b), the glassy carbon electrode modified with PMo_{12}-stabilized Pt nanoparticles exhibited electrocatalytic activity towards oxygen reduction. PMo_{12} may activate Pt in a manner analogous to tungsten oxides [67].

The growth of the multilayer network film consisting of Pt-PMo_{12} and PANI is evident from the increase of voltammetric peak currents (Fig. 8) recorded in the electrolyte following alternate immersions in Pt-PMo_{12} colloidal suspension and the anilinium solution (the latter

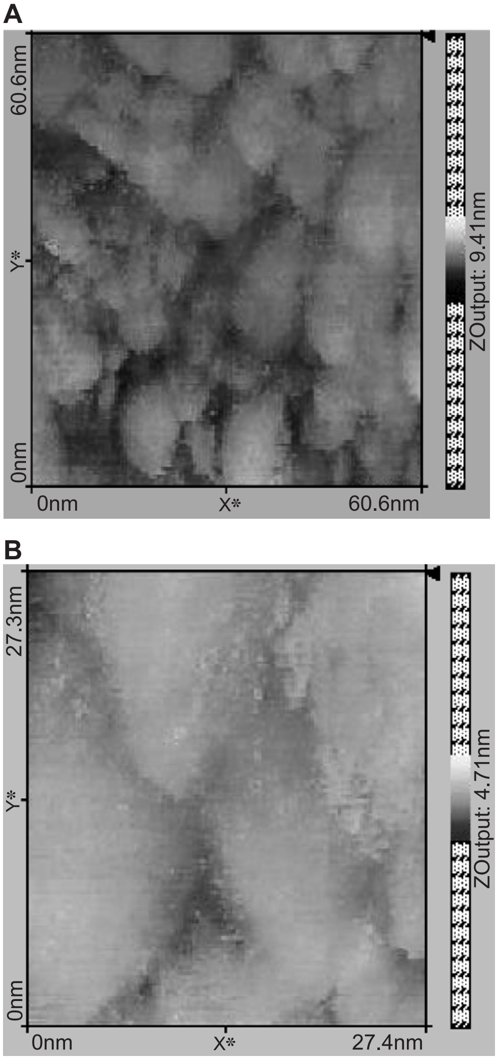

Fig. 7. STM examination of PMo_{12}-protected Pt nanoparticles self-assembled on glassy carbon. The images are taken at two different scales, larger (A) and smaller (B).

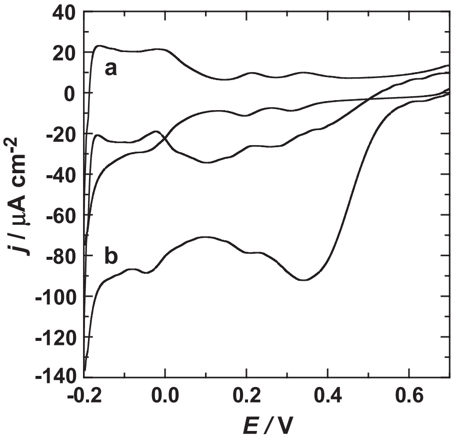

Fig. 6. Voltammetric behavior of glassy carbon electrode modified with a monolayer of PMo_{12}-protected Pt nanoparticles in 0.5 mol dm^{-3} H_2SO_4 saturated with (a) argon, and (b) air. Scan rate, 50 mV s^{-1}.

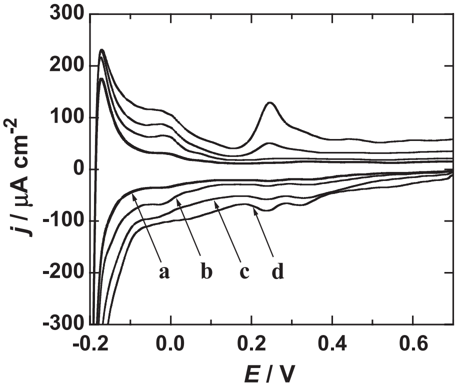

Fig. 8. Cyclic voltammetric responses of a network hybrid PMo_{12}-Pt/PANI film (on glassy carbon) recorded after processing through (a) one, (b) two, (c) three, and (d) four cycles of alternate treatments in the solutions of PMo_{12}-protected Pt and 0.07 mol dm^{-3} aniline in 0.5 mol dm^{-3} H_2SO_4. Electrolyte, 0.5 mol dm^{-3} H_2SO_4. Scan rate, 50 mV s^{-1}.

step was combined with the interfacial electropolymerization of PANI [9]). Apparently PMo_{12} (that is chemisorbed on Pt particles) is rigid and retains its anionic character that permits electrostatic attraction of positively charged PANI.

We monitored the reactivity of platinum nanocenters dispersed within network film towards reduction of dioxygen by recording voltammetric responses (Fig. 9) in 0.5 mol dm^{-3} H_2SO_4 solutions saturated with air (Curve b) and oxygen (Curve c). The results are consistent with the view that the PANI-linked PMo_{12}-protected Pt nanoparticles catalyzed reduction of oxygen in a manner analogous to metallic Pt. On the other hand, the voltammetric peaks for oxygen reduction appeared in Fig. 9 (Curves b and c) at somewhat less positive potentials in comparison to the data of Fig. 6 (Curve b) describing the reduction of oxygen at the glassy carbon electrode modified with a monolayer of PMo_{12}-stabilized Pt nanoparticles. Our preliminary rotating disk measurements indicate that, while the oxygen reduction was a diffusion-controlled process (at least up to 4900 rpm) in case of the system of Fig. 6 (Curve b), the interfacial electron-transfer kinetic control became apparent upon introduction of polymer layers. Further research is in progress along this line.

Although conducting polymers are known to be attractive matrices for dispersed platinum [68–70], the voltammetric peak potential at which oxygen was reduced in Fig. 9 (Curves b and c) is less positive when compared to the system's behavior under the analogous conditions but at platinized tungsten oxide [62]. It is reasonable to expect that this unfavorable potential shift, that is mentioned above, has resulted from the interfacial electropolymerization of inhibiting aniline monomer on the surface of PMo_{12}-stabilized Pt nanoparticles. No inhibition (negative potential shift for oxygen reduction) is observed [66] when nanoparticles are immobilized into the PANI film that has already been assembled in the polymerized form.

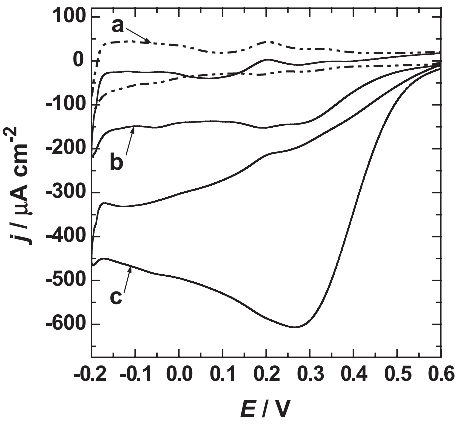

Fig. 9. Electrocatalytic reduction of oxygen at the network hybrid network hybrid PMo_{12}-Pt/PANI film of Fig. 8. Voltammetric responses were recorded in 0.5 mol dm^{-3} H_2SO_4 saturated with (a) argon, (b) air, and (c) dioxygen. Other parameters as for Fig. 6.

4. Conclusions

PMo_{12} undergoes strong spontaneous chemisorption on solid surfaces (e.g. glassy carbon, Pt). As yet we do not have direct proof for the true self-assembly process but our microgravimetric data, and the preliminary STM results of others [76], are consistent with the formation of a dense, robust, monolayer-type ultra-thin film of ordered heteropolymolybdate nanostructures. We also demonstrate the usefulness of the layer-by-layer approach to the fabrication of hybrid films composed of the heteropolyanion (e.g. PMo_{12}) monolayers and ultra-thin layers of conducting polymers (e.g. PANI). Although a concept of the preparation of composite films of polyoxometallates and conducting polymers is not new [71–75], our approach is based on electropolymerization of surface-confined monomer ions that are electrostatically attached and chemically attracted to a negatively charged self-assembled polyoxometallate (PMo_{12}) monolayer. The fact that PANI interlayers are electronically/ionically conducting in the potential range where the PMo_{12} layers are electroactive implies good electrical contact in the vertical dimension in the case of multilayer films. The latter property combined with reactivity of polyoxometallate redox centers could be of importance to the development of effective electrocatalytic systems.

An important issue is the feasibility of stabilization of platinum nanoparticles by protecting them through chemisorption of polyoxometallate (PMo_{12}) monolayers on their surfaces. The particles produce self-assembled layers on electrode surfaces, and they can be linked by via ultra-thin polymer (PANI) layers to form network films with highly reactive platinum centers (e.g. towards reduction of oxygen). The approach seems to provide a novel concept of assembling conducting polymers, polyoxometallates and metal nanoparticles into the network electrocatalytic structures.

Following examination of the literature and having in mind potential biochemical and medical applications, the highly functionalized nanostructured architectures entrapping Keggin-type polyoxometallates can effectively be used as constrained environments for the encapsulation of guest molecules (e.g. using the protein coats of viruses as hosts) [77] with potential applications in drug delivery and catalysis, for the assembling of biosensors (e.g. for glucose [78]), specific interaction with nucleic acids [79] or bilayer lipid membranes [80], polyoxometallate-mediated inactivation of DNA polymerases [81], catalytic oxidation of NADH [82], as well as anticancer and antiviral systems [83,84].

Acknowledgement

This work was supported by Ministry of Science (Poland) under the State Committee for Scientific Research

(KBN) grants 7 T09A 05426 and 4 T09A 12225 (doctoral). KM was supported in part by the University of Warsaw under BW-1602/9/2003. MCh appreciates the stipend from Foundation for Polish Science, FNP.

References

[1] J.H. Fendler (Ed.), Nanoparticles and Nanostructured Films, Wiley-VCH, Weinheim, Germany, 1998.
[2] A. Ulman, An Introduction to Ultrathin Organic Films from Langmuir-Blodgett to Self-Assembly, Academic Press, New York, 1991.
[3] L.H. Dubois, R.G. Nuzzo, Annu. Rev. Phys. Chem. 43 (1992) 437.
[4] A. Ulman, Chem. Rev. 96 (1996) 1533.
[5] R.J. Willicut, R.M. McCarley, J. Am. Chem. Soc. 116 (1994) 10824.
[6] G. Zotti, G. Schiavon, S. Zachin, A. Berlin, G. Pagani, A. Canavesi, Langmuir 13 (1997) 2694.
[7] I. Turyan, D. Mandler, J. Am. Chem. Soc. 120 (1998) 10733.
[8] A. Fikus, W. Plieth, D. Appelhans, D. Ferse, H.-J. Adler, B. Adolphi, F.-J. Schmitt, J. Electrochem. Soc. 146 (1999) 4522.
[9] P.J. Kulesza, M. Chojak, K. Miecznikowski, A. Lewera, M.A. Malik, A. Kuhn, Electrochem. Commun. 4 (2002) 510.
[10] C.A. Mirkin, Inorg. Chem. 39 (2000) 2258.
[11] L. Carrette, K.A. Friedrich, U. Stimming, Chem. Phys. Chem. 1 (2000) 162.
[12] S. Park, P. Yang, P. Corredor, M.J. Weaver, J. Am. Chem. Soc. 124 (2002) 2428.
[13] L. Charette, K.A. Friedrich, U. Stimming, Chem. Phys. Chem. 1 (2000) 162.
[14] P. Waszczuk, J. Solla-Gullon, H.-S. Kim, Y.Y. Tong, V. Montiel, A. Aldaz, A. Wieckowski, J. Catal. 203 (2001) 1.
[15] J. McBreen, S. Mukerjee, in: A. Wieckowski (Ed.), Interfecial Electrochemistry, Marcel Dekker, New York, 1999, p. 895.
[16] M.T. Reetz, M. Lopez, W. Grunert, W. Vogel, F. Mahlendorf, J. Phys. Chem., B 107 (2003) 7414.
[17] A.C. Templeton, W.P. Wuelfing, R.W. Murray, Acc. Chem. Res. 33 (2000) 27.
[18] M. Brust, M. Walker, D. Bethell, D.J. Schiffrin, R. Whyman, J. Chem. Soc., Chem. Commun. (1994) 801.
[19] S.L. Horswell, I.A. O'Neil, D.J. Schiffrin, J. Phys. Chem., B 105 (2001) 941.
[20] J.M. Petroski, T.C. Green, M.A. El-Sayed, J. Phys. Chem., A 105 (2001) 5542.
[21] F.P. Zamborini, M.C. Leopold, J.F. Hicks, P.J. Kulesza, M.A. Malik, R.W. Murray, J. Am. Chem. Soc. 124 (2002) 8958.
[22] D. Bethell, M. Brust, D.J. Schiffrin, C. Kiely, J. Electroanal. Chem. 409 (1996) 137.
[23] S.L. Horswell, I.A. O'Neil, D.J. Schiffrin, J. Phys. Chem., B 105 (2001) 941.
[24] R.C. Mucic, J.J. Storhoff, R.L. Lestsinger, C.A. Mirkin, Nature 382 (1996) 607.
[25] J.J. Shiang, J.R. Heath, C.P. Colier, R.J. Saykally, J. Phys. Chem., B 102 (1998) 3425.
[26] T.E. Mallouk, H.-N. Kim, P.-J. Ollivier, S.W. Keller, Ultrathin Films Based on Layered Inorganic Solids, vol. 7, Pergamon Press, Oxford, 1996.
[27] G. Decher, Y. Lvov, J. Schmitt, Thin Solid Films 244 (1994) 772.
[28] E.R. Kleinfeld, G.S. Fergusson, Chem. Mater. 7 (1995) 2327.
[29] S.W. Keller, H.N. Kim, T.E. Mallouk, J. Am. Chem. Soc. 116 (1994) 8817.
[30] I. Moriguchi, J. Fendler, Chem. Mater. 10 (1998) 2205.
[31] D. Ingersoll, P.J. Kulesza, L.R. Faulkner, J. Electrochem. Soc. 141 (1994) 140.
[32] A. Kuhn, F.C. Anson, Langmuir 12 (1996) 5481.
[33] L. Cheng, L. Niu, J. Gong, S. Dong, Chem. Mater. 11 (1999) 1465.
[34] L. Cheng, G.E. Pacey, J.A. Cox, Electrochim. Acta 46 (2001) 4223.
[35] R. Sfez, L. De-Zhong, I. Turyan, D. Mandler, S. Yitzchaik, Langmuir 17 (2001) 2556.
[36] M. Ge, B. Zhong, W. Klemperer, A.A. Gewirth, J. Am. Chem. Soc. 118 (1996) 5812.
[37] C. Sun, J. Zao, H. Xu, Y. Sun, X. Zhang, J. Shen, J. Electroanal. Chem. 435 (1997) 63.
[38] D. Martel, A. Kuhn, P.J. Kulesza, M. Galkowski, M.A. Malik, Electrochim. Acta 46 (2001) 4197.
[39] M. Lira-Cantu, P. Gomez-Romero, Chem. Mater. 10 (1998) 698.
[40] A. Kuhn, N. Mano, C. Vidal, J. Electroanal. Chem. 462 (1999) 187.
[41] P.J. Kulesza, K. Miecznikowski, M.A. Malik, M. Galkowski, M. Chojak, K. Caban, A. Wieckowski, Electrochim. Acta 46 (2001) 4065.
[42] S. Pruneanu, E. Csahok, V. Kertesz, G. Inzelt, Electrochim. Acta 43 (1998) 2305.
[43] G. Ybarra, C. Moina, M.I. Florit, D. Posadas, Electrochem. Solid-State Lett. 3 (2000) 330.
[44] A. Neudeck, A. Petr, L. Dunsch, J. Phys. Chem., B 103 (1999) 912.
[45] A. Smie, J. Heinze, Angew. Chem., Int. Ed. Engl. 36 (1997) 36.
[46] A. Boyle, E. Genies, M. Lapkowski, Synth. Met. 28 (1989) C769.
[47] M.-C. Bernard, A. Hugot-LeGoff, S. Joiret, N.N. Dinh, N.N. Toan, Synth. Met. 102 (1999) 1383.
[48] M. Granstrom, M. Berggren, O. Inganas, Science 267 (1995) 1479.
[49] F. Sundfords, J. Bobacka, A. Ivaska, A. Lewenstam, Electrochim. Acta 47 (2002) 2245.
[50] K.V. Sarathy, G. Raina, R.T. Yadav, G.U. Kulkarni, C.N.R. Rao, J. Phys. Chem., B 101 (1997) 9876.
[51] M.J. Hostetler, C.J. Zhong, B.K.H. Yen, J. Anderegg, S.M. Gross, N.D. Evans, M. Porter, R.W. Murray, J. Am. Chem. Soc. 120 (1998) 9396.
[52] S.L. Horswell, C.J. Kiely, I.A. O'Neil, D.J. Schiffrin, J. Am. Chem. Soc. 121 (1999) 5573.
[53] H. Perez, R.M.L. de Souza, J.P. Pradeau, P.-A. Albouy, Chem. Mater. 13 (2001) 1512.
[54] M.T. Reetz, M. Lopes, W. Grunert, W. Vogel, F. Mahlendorf, J. Phys. Chem., B 107 (2003) 7414.
[55] A. Miyazaki, Y. Nakano, Langmuir 16 (2000) 7109.
[56] T.S. Ahmadi, Z.L. Wang, T.C. Green, A. Henglein, M.A. El-Sayed, Science 272 (1996) 1924.
[57] C. Rocchiccioli-Deltcheff, M. Fournier, R. Franck, R. Thouvenot, Inorg. Chem. 22 (1983) 207.
[58] A.J. Bard, L.R. Faulkner, Electrochemical Methods: Fundamentals and Applications, 2nd ed., Wiley, 2001.
[59] P.J. Kulesza, M.A. Malik, in: A. Wieckowski (Ed.), Interfacial Electrochemistry, Ch. 37 "Solid-State Voltammetry", Marcel Dekker, New York, 1999.
[60] L. Adamczyk, P.J. Kulesza, K. Miecznikowski, B. Palys, M. Chojak, D. Krawczyk, J. Electrochem. Soc. (submitted for publication).
[61] P.J. Kulesza, L. Adamczyk, D. Krawczyk, O. Makowski, K. Miecznikowski, M. Ocypa, M. Chojak, Proceeding Volume ECS (in press).
[62] P.J. Kulesza, L.R. Faulkner, J. Am. Chem. Soc. 110 (1988) 490.
[63] Y.Q. Fu, T.R. Zhang, C.Q. Sun, J. Solid State Electrochem. 7 (2002) 25.
[64] P. Wang, X.P. Wang, G.Y. Zhu, Electroanalysis 12 (2000) 1493.
[65] P.J. Kulesza, M. Chojak, K. Karnicka, K. Miecznikowski, A. Piranska, 204th Meeting of The Electrochemical Society, Orlando, USA, 2003, Abstract 159.
[66] P.J. Kulesza, M. Chojak, K. Karnicka, K. Miecznikowski, B. Palys, A. Lewera, A. Wieckowski, Chem. Mater. (submitted for publication).
[67] P.J. Kulesza, L.R. Faulkner, J. Electroanal. Chem. 259 (1989) 81.
[68] C. Coutanceau, M.J. Croissant, T. Napporn, C. Lamy, Electrochim. Acta 46 (2000) 579.
[69] S.Q. Liu, Z.Y. Tang, E.K. Wang, S.J. Dong, Electrochem. Commun. 2 (2000) 800.
[70] M. Hepel, J. Electrochem. Soc. 145 (1998) 124.

[71] M. Lapkowski, G. Bidan, M. Fournier, Synth. Met. 41 (1991) 407.
[72] G. Bidan, E.M. Genies, M. Lapkowski, Synth. Met. 31 (1989) 327.
[73] G. Bidan, M. Lapkowski, J.P. Travers, Synth. Met. 28 (1989) C113.
[74] B. Keita, D. Bouaziz, L. Nadjo, J. Electroanal. Chem. 255 (1988) 303.
[75] G. Bidan, E.M. Genies, M. Lapkowski, J. Electroanal. Chem. 251 (1988) 533.
[76] D. Martel, PhD Thesis, University of Bordeaux, France (2000).
[77] T. Douglas, M. Young, Nature 393 (1998) 152.
[78] G.L. Turdean, A. Curulli, I.C. Popescu, C. Rosu, G. Palleschi, Electroanalysis 14 (2002) 1550.
[79] J. Peng, W.Z. Li, X.L. Zhao, Z.G. Han, B.Q. Huang, Chem. Res. Chin. Univ. 20 (2004) 6.
[80] J.G. Wang, L. Wang, S.Q. Liu, H.J. Han, W.M. Huang, E.K. Wang, Biophys. Chemist. 106 (2003) 31.
[81] S.G. Sarafianos, U. Kortz, M.T. Pope, M.J. Modak, Biochem. J. 319 (1996) 619.
[82] B. Keita, K. Essaadi, A. Belhouari, L. Nadjo, R. Contant, Y. Justum, C. R. Acad. Sci., Sér. IIc Chim. 1 (1998) 343.
[83] S. Lis, Acta Phys. Pol., A 90 (1996) 275.
[84] J.T. Rhule, C.L. Hill, D.A. Judd, Chem. Rev. 98 (1998) 327.